Proceedings of the
Annual Stability Conference
Structural Stability Research Council
St. Louis, Missouri, April 16-20, 2013

Stability of cold-formed steel compression members under thermal gradients

J.C. Batista Abreu[1], B.W. Schafer[2]

Abstract

This paper explores the elastic stability of concentrically loaded cold-formed steel (CFS) members subjected to non-uniform temperature distributions. The main objectives of this study are to show the evolution of the buckling loads and modes due to fire action, and explore the finite strip method as an alternative technique for evaluating the stability of CFS members subjected to thermal load. During a fire, elevated temperatures modify the thermal and mechanical properties of CFS, altering the material strength and member stiffness, so that the load-carrying capacity is reduced. Since fire causes non-uniform and time-varying thermal loads, temperature gradients are developed on the structure and its members, leading to unsymmetric member response even when the applied load is uniformly distributed and initial geometric imperfections are negligible. In addition, the instabilities of CFS members are associated with the temperature distributions that such members experience. For instance, a column dominated by local buckling at ambient temperature could present a local-distortional buckling interaction under a fire generated temperature field. Computational analyses are performed to determine the temperature distribution on the structure over time, considering a standard fire curve as the input thermal condition. Sequentially coupled mechanical analyses are used to investigate the member stability associated with thermal gradients, using the finite element method. Approximate results, obtained from the more efficient finite strip method, are compared against the finite element solutions.

1. Introduction

Cold-formed steel (CFS) is extensively used for civil applications in residential, commercial and industrial buildings. CFS structures have gained popularity because of their easy production, high strength to weight ratio, economy in transportation, and fast installation. Since CFS sections are increasingly used as primary structural members, they are required to satisfy certain requirements, including fire resistance.

[1] Graduate Research Assistant, Department of Civil Engineering, Johns Hopkins University, jbatist1@jhu.edu
[2] Professor and Chair, Department of Civil Engineering, Johns Hopkins University, schafer@jhu.edu

The stability response of thin-walled CFS member under fire conditions can be evaluated computationally, if grounded in experimental knowledge of the mechanical behavior. Structural behavior depends on the temperature field applied to the member (which is commonly non-uniform), the temperature dependent mechanical properties, and the resulting deformation field due to thermal action. In general, to predict the load-carrying capacity of CFS members the Direct Strength Method (DSM) has been evaluated and found to be adequate, even for elevated temperatures. However, existing evaluations of DSM are based on only a few predefined temperature distributions; while, the expected temperature distributions depend on the fire scenario, and are time-varying. Multiple fire scenarios are adopted in this research, considering the evolution of the thermal gradient over time, with the objective of studying the degradation of the local, distortional and global buckling loads, i.e. the key inputs in DSM. The results are intended for future DSM-based predictions of the axial capacity of CFS compression members at an expected fire resistance rating.

2. Material properties of CFS at elevated temperatures

The behavior of CFS structures under fire conditions depends on the temperature distribution in the structural members and this, in turn, governs the thermal and mechanical properties of the material. In a real fire scenario, temperature is not uniform in the member, and so the material strength is potentially non-uniform throughout the cross-section, and along the member length. However, steel mass density remains fairly constant around 7850 kg/m^3 at the temperature range expected during a fire, showing a slight decrease (about 5%) at 1200°C (Costes 2004).

2.1 Thermal properties

To characterize structural behavior under fire conditions it is necessary to understand the temperature dependence of the thermal and mechanical properties of CFS. The first stage consists in understanding how heat transfer is modified while the temperature of the material rises. The heat capacity of carbon steel increases with temperature before a phase change occurs in the molecular structure, at about 730°C. At a similar temperature range, the ability to conduct heat decreases which means that the material better resists heat flow at higher temperatures. Differential temperature also induces thermal strains in the material. This is associated with the thermal expansion coefficient, which increases with temperature. Variation of the specific heat, thermal conductivity, and thermal expansion coefficient with temperature are shown in Fig. 1, as per Eurocode 3 Part 1.2 (1993).

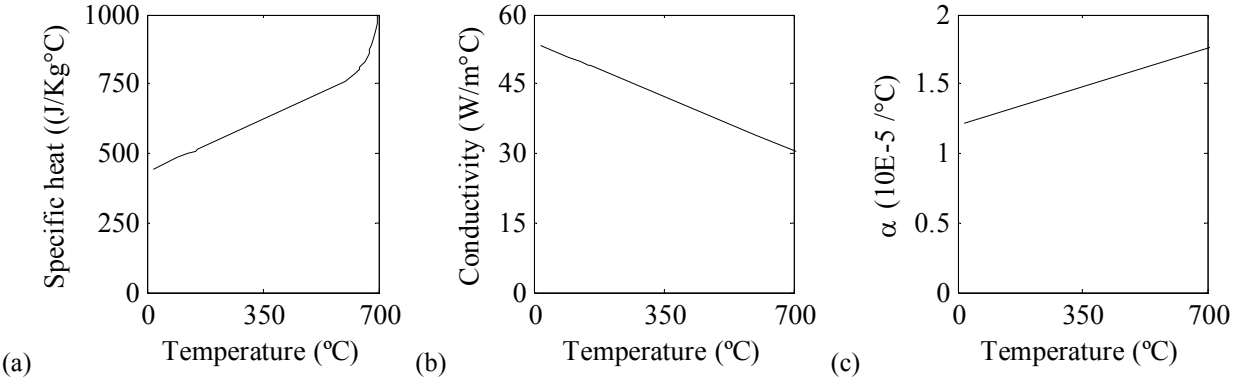

Figure 1: (a) Specific heat, (b) thermal conductivity and (c) thermal expansion coefficient of carbon steel at high temperatures (Eurocode 3 Part 1.2 1993)

2.2 Mechanical properties

The degradation of mechanical properties determines the resistance of a structural member under mechanical and thermal loads. Several equations have been proposed to predict material response at elevated temperatures. Generally, they are found in the literature as a ratio of a given mechanical property at elevated temperatures with respect to the ambient condition. Such equations are based on scattered experimental data, as shown in Fig. 2. Reduction factors differ among authors; although, in general, the elastic modulus, yield strength and ultimate strength decay with increasing temperature. The differences are generally related to the test method used (i.e. transient or steady-state), test setup, instrumentation used to measure strains, the material grade of the specimen, the chemical composition of the steel, and the criteria used to compute elastic modulus and identify the yield strength. For instance, reduction factors for yield strength depend on the steel grade (see Fig. 3-a). Also, reduction factors from transient state tests are lower than those obtained through steady-state tests (see Fig. 3-b). Most existing studies are based on reduction factors from steady-state tests as they are easier to conduct, despite the fact that transient state reductions are more severe and generally considered more realistic.

Fig. 4 provides the mechanical properties used to simulate the structural behavior of CFS compression members under thermal load as proposed by Kankanamge and Mahendran (2011). The elastic modulus and yield strength at ambient temperature are 203,500 MPa (29,500 ksi) and 345 MPa (50 ksi), respectively. Figs. 4-a and 4-b also show the reduction factors for steel from AISC (2005) and Eurocode 3 Part 1.2 (1995). Both design codes provide similar reduction factors for elastic modulus of structural steel, which (in general) are greater than that of cold-formed steel. Poisson's ratio of steel is commonly considered to be temperature independent (Kaitila 2002). However, Clark (1953) showed a slight variation of Poisson's ratio with temperature around 0.3, which is a common value used for computations at ambient and elevated temperatures (see Fig.4-c). Experimental data is used to predict temperature dependent stress-strain relationships and generate stress-plastic strain curves to define plasticity models for computational analysis (see Fig. 5).

3. Temperature distribution on CFS columns subjected to heating thermal load

In light steel framing systems, CFS studs (or joists) are usually sheathed with parallel layers of board. During a fire, heat is transferred to the studs through these layers, resulting in a non-uniform temperature distribution in the member cross-section and along its length. Even under controlled conditions of thermal action, columns develop a non-uniform temperature distribution (Almeida et al. 2012). This non-uniformity is maintained in the studs until their failure when subjected to thermal load from one side (Alfawakhiri and Sultan 2001). This fact influences the behavior and failure mode of the structure. For instance, members subjected to axial compression under non-uniform fire action behave as beam-columns due to bending moments produced by: (1) the thermal bowing effect in long columns caused by the different level of expansion between the exposed and unexposed faces of the member, and (2) the nonlinear stress distribution in the cross-section, since the stress-strain relationship is temperature dependent and plasticity occurs first in the region with higher temperature under uniform external load. Consequently, the fire scenario can have a significant impact on the structural response.

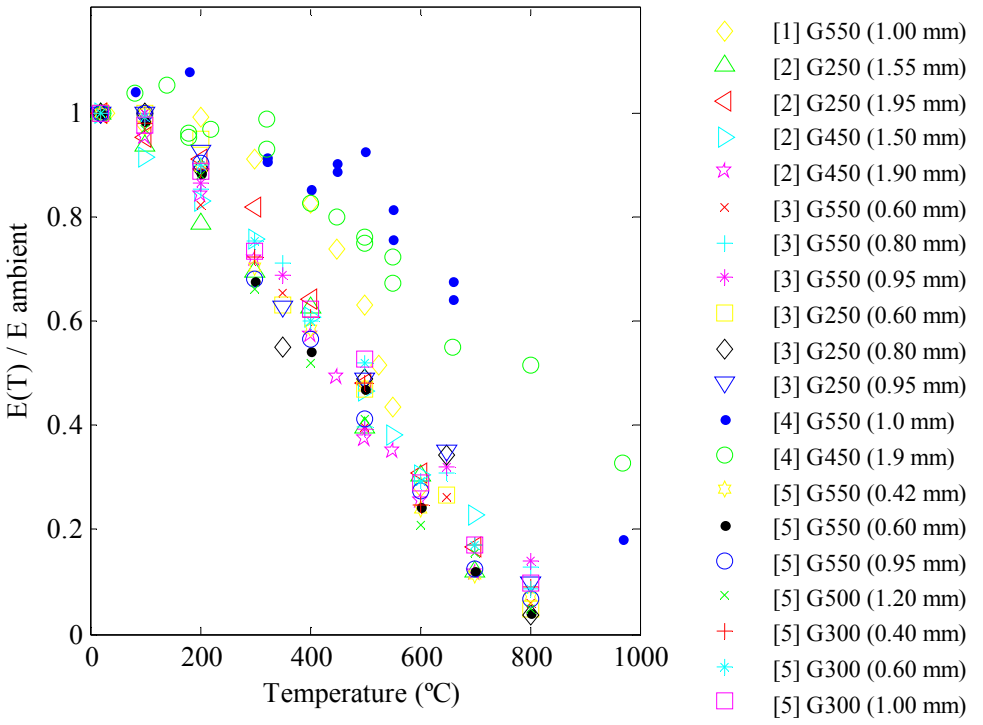

Figure 2: Reduction factors for elastic modulus from steady-state testing by: [1] Wei and Jihong (2012), [2] Kankanamge and Mahendran (2011), [3] Ranawaka and Mahendran (2009), [4] Chen and Young (2007), and [5] Lee and Mahendran (2003). Legend: [author] steel grade (specimen thickness)

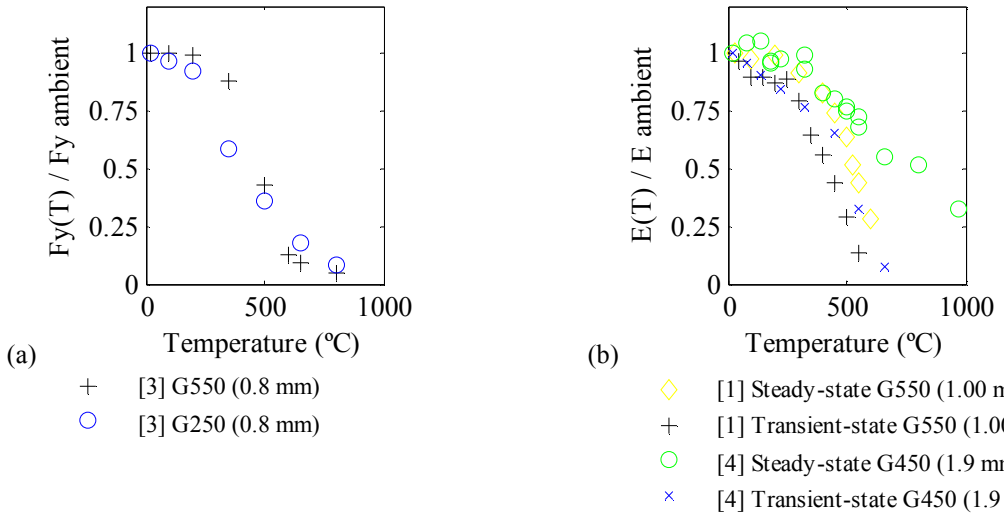

Figure 3: Variation of reduction factors for CFS at elevated temperatures with (a) steel grade and (b) test method, by: [1] Wei and Jihong (2012), [3] Ranawaka and Mahendran (2009) and [4] Chen and Young (2007). Legend: [author] steel grade (specimen thickness)

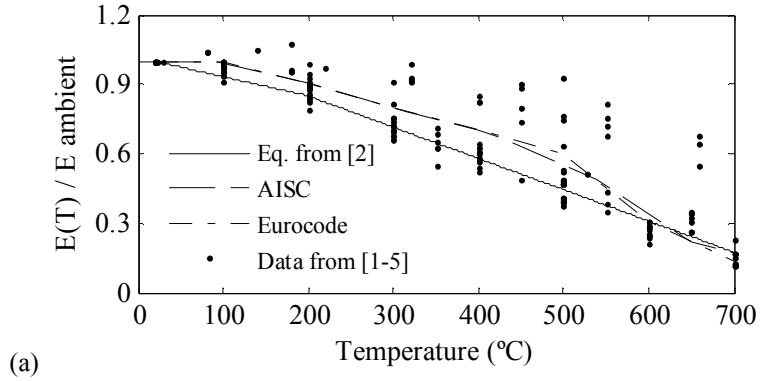

(a)

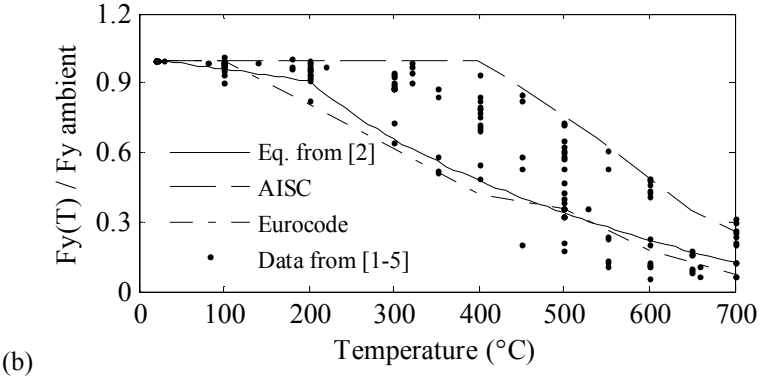

(b)

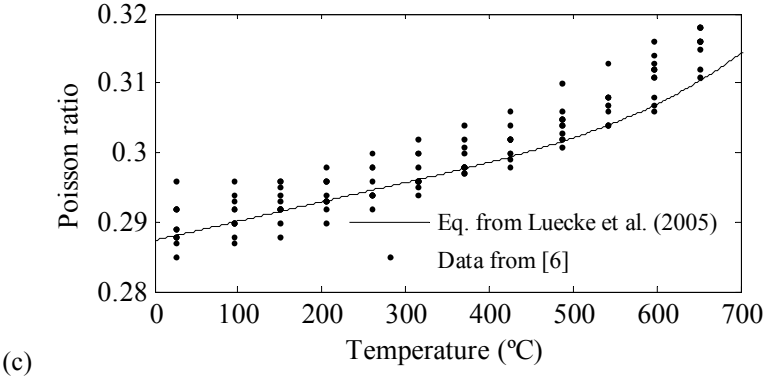

(c)

Figure 4: Reduction factors for (a) elastic modulus and (b) yield strength, and (c) Poisson's ratio of steel
Strength data from [1] Wei and Jihong (2012), [2] Kankanamge and Mahendran (2011), [3] Ranawaka and Mahendran (2009), [4] Chen and Young (2007), [5] Lee and Mahendran (2003), and Poisson's ratio data from [6] Clark (1953)

3.1 Fire scenarios

Multiple fire scenarios are likely to occur in a given building. For numerical simulations, these scenarios are usually associated with a time-temperature curve such as the Standard, Hydrocarbon, External or Parametric fire curves. Standard fire curves are commonly used to determine the fire resistance of structural members and assemblies. These standard fires are temporal quantitative temperature representations, based on fuel load found in conventional buildings at the beginning of the 20th century (Collette 2007). External fire curves are meant to describe the temporal temperature variation in the outside of an external wall, while Hydrocarbon curves describe the case when hydrocarbons are the main fuel load during a fire. Parametric fire curves comprise specific factors such as ventilation, fuel load, compartment size

and its thermal properties to represent a post-flashover compartment fire in a more realistic manner. Since this work aims to study the evolution of the buckling loads and modes of CFS studs due to temperature increase, the Standard fire curve was utilized (see Fig. 6) as a simple first start point. In the models, temperature was increased up to 700°C, since beyond this point material strength is low, and the member is no longer able to carry a significant load.

3.2 Heat transfer analysis

To simulate the evolution of the temperature field on the studied CFS studs, heat transfer analyses were performed using quadrilateral heat transfer shell elements of type DS4 in Abaqus (2009). This is a 4-node heat transfer quadrilateral shell element. The web, flanges and lips were discretized into 16, 8 and 4 rectangular elements, respectively. Temperature dependence of the conductivity and specific heat were specified, as per Fig. 1. The nonlinear heat transfer problem was solved in Abaqus, to obtain the transient response of the studs subjected to thermal load.

Fig. 7 provides the evolution of the temperature difference and ratio between the exposed and unexposed flanges of a CFS stud over time. The thermal load corresponds to the Standard fire curve, acting directly on one flange of the member. The figure shows that the temperature difference between flanges grows quickly, up to 365°C even though the web of the member is just 2.5 inches wide. The temperature ratio between flanges grows rapidly since only one flange is directly exposed to fire load. After this peak, the temperature difference decreases at a lower rate, so the heat is transferred to the unexposed elements and the global temperature tends to stabilize. Results from the heat transfer analyses are followed by sequentially coupled mechanical analyses, including eigenvalue buckling and collapse analyses. The temperature distribution over time was utilized as a predefined field for further perturbation and stress analyses.

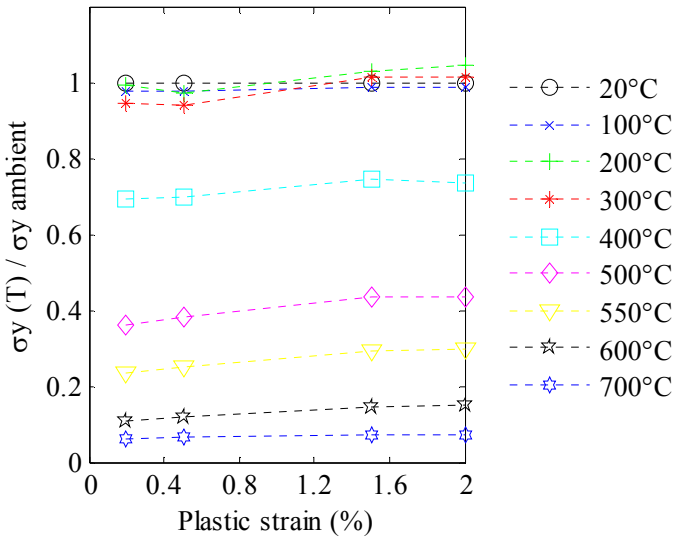

Figure 5: Yield strength reduction factors at various strain levels for steel G450, by Kankanamge and Mahendran (2011)

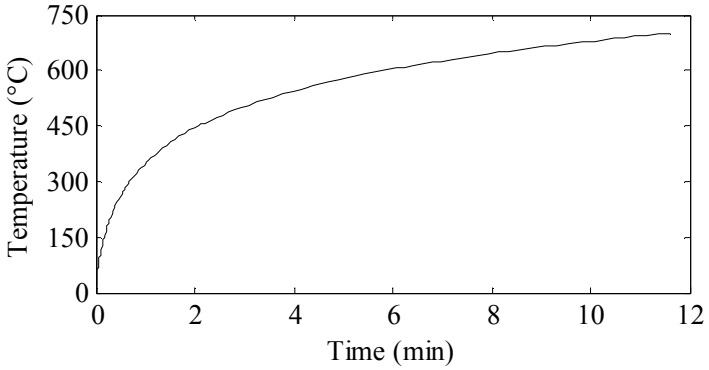

Figure 6: ISO 834 standard fire curve

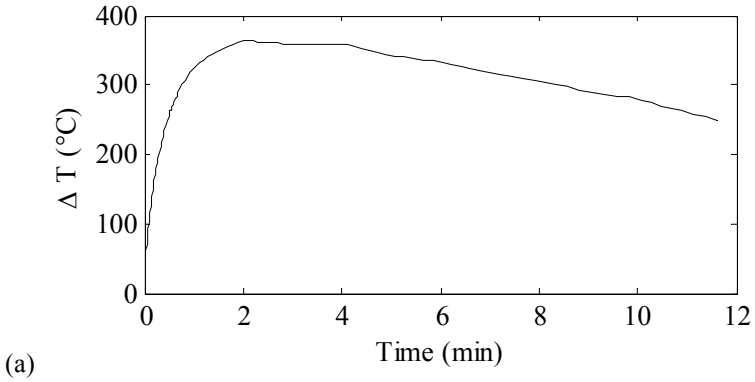

(a)

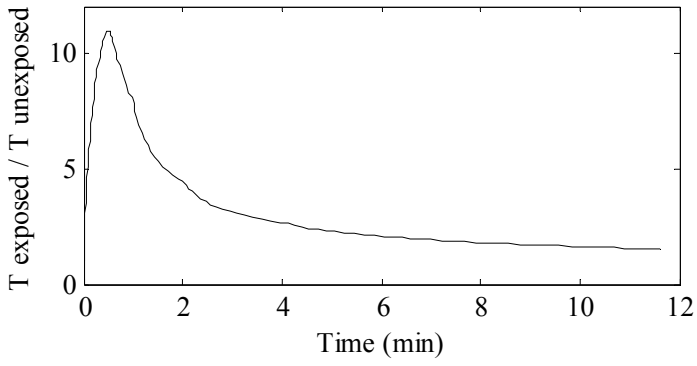

(b)

Figure 7: (a) Temperature difference and (b) temperature ratio between exposed and unexposed flanges of a 250S137-68 CFS stud with thermal load (Standard fire curve) on one flange

4. Elastic buckling analysis

Several authors (Feng et al. 2003b, Chen and Young 2006, Shahbazian and Wang 2011a, 2011b and 2012) have shown that the Effective Width Method and the Direct Strength Method are both suitable to compute column strength at elevated temperatures. Most studies on the behavior of CFS compression members at elevated temperatures have focused on the response to uniform temperatures (Lee 2004, Chen and Young 2006, Ranawaka and Mahendran 2010). Reducing mechanical properties may be enough to conservatively predict the column strength for the idealized scenario in which the temperature is uniform. However, the buckling behavior of thin-walled members becomes complex at high temperatures due to the non-uniform thermal load, the resulting non-uniformity of the material properties, and thermal bowing.

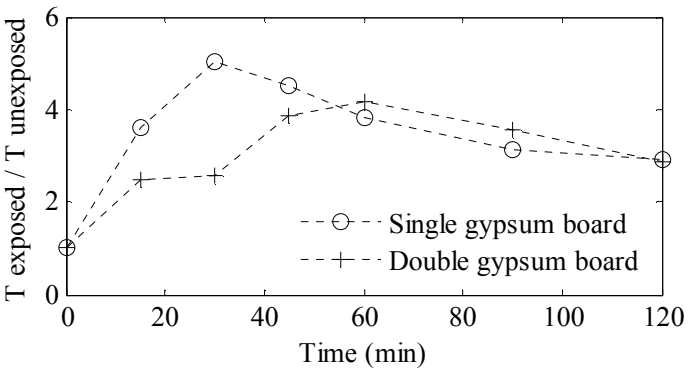

Figure 8: Temperature ratio between exposed and unexposed faces of a 100x54x15x1.2 lipped channel with thermal load (cellulosic fire curve) on one flange from Feng et al. (2003c)

Buckling curves were proposed by Shahbazian and Wang (2011a, 2011b and 2012), considering that one flange is exposed to thermal load. The proposed curves correspond to three temperature profiles, assuming that the temperature ratios between the exposed and unexposed flanges are 3, 2 and 1.5 at 120 minutes. Experimental data has shown that the temperature ratio is time dependent (see Fig. 8) and potentially quite different than the assumed values (see Fig. 7-b). This assumption also implies that time (or fire resistance) is no longer related to the axial capacity since the temperature profiles are not associated to time of fire exposure. Therefore, this paper presents a procedure to ultimately generate DSM buckling curves associated with the fire exposure time, thus member capacity and fire resistance are directly related to each other.

The degradation of the mechanical properties due to fire affects the elastic stability of the thin-walled members so that the local, distortional and global buckling loads are lessened and new buckling mode interactions are also possible. For instance, experimental results by Feng et al. (2003a) qualitatively show that short columns without holes dominated by distortional failure mode at temperatures below 400°C exhibit a local-distortional-flexural buckling interaction at higher temperatures. Similarly, the same short columns with holes dominated by local buckling at temperatures below 400°C failed in distortional buckling at higher temperatures. This evolution of modal interaction was described quantitatively by Li et al. (2012), through modal identification using the constrained finite strip method.

In addition, the response of a CFS structure under fire is also influenced significantly by the boundary conditions of the member, both thermal and mechanical. For instance, the interaction between a CFS stud and the gypsum board attached to it plays an important role, since the board-fastener system defines the level of lateral restraint for the stud. This restraint may be eventually lost at high temperatures due to calcination of the gypsum board (Gerlich 1995). Further, the fasteners themselves play an important role in transmitting the thermal demands to the stud. In addition, the buckling failure mode is also influenced by interior insulation in CFS assemblies (Alfawakhiri and Sultan 2001, Kodur and Sultan 2001).

4.1 Computational models

The following computational models simulate the effect of non-uniform thermal load on axially loaded CFS studs. The selected geometry corresponds to a 250S137-68 (AISI S200) lipped channel section. The CFS studs are modeled as pin ended compression members and analyzed

using the finite element method and finite strip method, utilizing Abaqus and CUFSM, respectively. In all cases the web, flanges and lips were discretized into 16, 8 and 4 rectangular elements, respectively. In Abaqus, linear quadrilateral shell elements of type S4 were used for structural analysis and DS4 for thermal analysis. In CUFSM, the constrained finite strip method was utilized to identify the minimum local, distortional and global buckling loads and corresponding lengths, for the first buckling mode.

The elastic buckling loads were computed at multiple fire scenarios and several times during fire exposure. The analysis considered the degradation of mechanical properties with increasing temperature, thus the non-uniform material strength and shift of center of resistance due to thermal action were taken into account. Buckling loads were disaggregated into local, distortional and global components to build time (or temperature) dependent curves showing the degradation of each buckling load.

To recreate multiple temperature profiles on the steel stud, three main cases were considered, in which (i) one flange, (ii) the web, or (iii) the lips are directly exposed to the thermal load (i.e. the Standard fire curve). The first model illustrates the case in which fire in a compartment directly affects one side of a CFS wall. First, heat is transferred to one flange and then it is spread to the whole steel member. The temperature distribution on the cross-section is illustrated in Fig. 9-a, where the bottom flange is subjected to uniform thermal load. Therefore, the web, top flange and lips show a slightly nonlinear temperature distribution. Feng et al. (2003b) showed that assuming uniform temperature in the flange and lips, and linear variation through the web height provides a good approximation of the column strength response. The other temperature profiles are illustrated in Fig. 9-b and c.

The buckling loads of the lipped channel were computed as a function of time, since the temperature distribution evolves while heat is transferred. Figs. 9-d, g and j show the degradation of local, distortional and global buckling loads, respectively. Each time of the analysis is related to the temperature distribution obtained through the transient heat transfer analysis as the member undergoes the Standard fire. Elastic buckling results were obtained with finite element analysis (using Abaqus) and finite strip analysis (using CUFSM), both with the same number of elements in the cross-section. When the web or the lips are directly exposed to the thermal load, degradation of the local, distortional and global buckling loads are provided in Figs. 9-e, h and k for the model with an exposed web, and Figs. 9-f, i and l for the model with exposed lips. If thermal bowing is (or can be) neglected, these curves can provide the column strength corresponding to a certain time (or fire resistance) using DSM. Thus the method allows explicit relation between the member strength and fire resistance.

4.2 Comparison of buckling loads and modes

Fig. 10 provides the normalized buckling loads with respect to the ambient buckling capacity over time, for the different fire scenarios. Local, distortional and global buckling loads are degraded the greatest when the web is the element directly exposed to thermal load, especially for local buckling since elevated temperatures weaken this slender thin-walled element which is prone to plate-like deformations. Also, the temperature increases fastest when the web is the element exposed to fire since it is the wider element, thus an earlier degradation of buckling loads is observed. Of course, in most design scenarios this would be an unusual thermal demand.

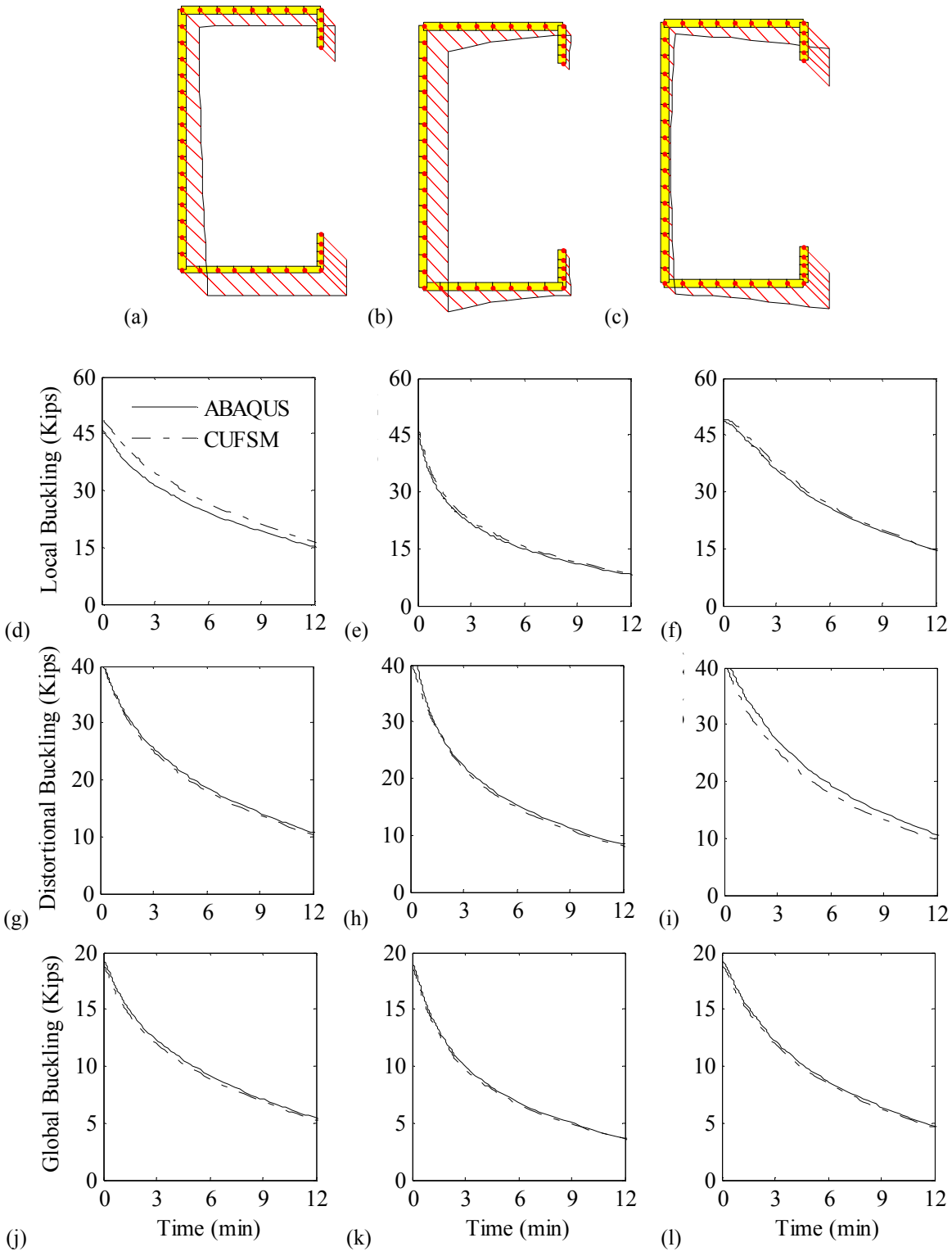

Figure 9: (a), (b) and (c) sketches of the temperature distributions in the cross-section, (d), (e) and (f) degradation of local buckling load, (g), (h) and (i) degradation of distortional buckling load, and (j), (k) and (l) degradation of global buckling load when the bottom flange, web or lips are directly exposed to the thermal load, respectively

In general, the rate of degradation of buckling loads decreases over time for the thermal load imposed. The effects of the thermal load acting on one flange or the lips are comparable in terms of reduction of the buckling loads; surprising, since the area of the flange is four times that of the lip. However, the local and distortional buckling modes show asymmetric deformations when one flange is directly exposed to the thermal load, i.e., the thermally loaded flange exhibits larger deflections.

A slight variation of the local and distortional half-wavelengths is observed for the different temperature distributions over time. Table 1 provides the average half-wavelength for each buckling mode, according to the fire scenario. The global buckling load was computed at a half-wavelength of 762 mm (30 in).

Stronger mode interactions are observed during the time (temperature) exposure than elastic buckling response at ambient temperature. Fig. 11 provides the local and distortional mode shapes at initial (Fig. 11-a) and final (Fig. 11-c) stages of fire action when material degradation is approximately uniform in the cross-section. Meanwhile, at intermediate stages (Fig. 11-b), the mode shapes are asymmetric and the mode corresponding to the minimum local buckling load shows distortion on the exposed flange due to the thermal gradient on the cross-section and the considerable degradation of the mechanical properties in this element. In this case, no local minimum was observed in the FSM signature curve. Also, an additional minimum for local buckling may appear in the signature curve when the thermal load severely degrades the elastic modulus (at very high temperatures).

The minimum buckling mode may also change from local to distortional and vice versa over the life of the fire. This transition was observed when the thermal load was imposed on the web of the lipped channel. As shown in Fig. 12-b, the minimum elastic buckling mode is local, between 16 and 24 minutes under thermal action. Otherwise, the minimum mode is always distortional (Figs. 12-a and 12-c). Both modes must still be considered in design (especially when elastic local buckling is lower than distortional) but the example illustrates the differing sensitivity of the modes to the thermal demand. In all cases, large channels [762 mm, 30 in.] exhibited flexural-torsional buckling.

Table 1: average half wavelength

Buckling mode	Element(s) directly exposed to fire		
	Flange	Web	Lips
Local	2.02”	1.97”	2.06”
Distortional	7.84”	8.76”	7.70”
Global	30.02”	30.02”	30.02”

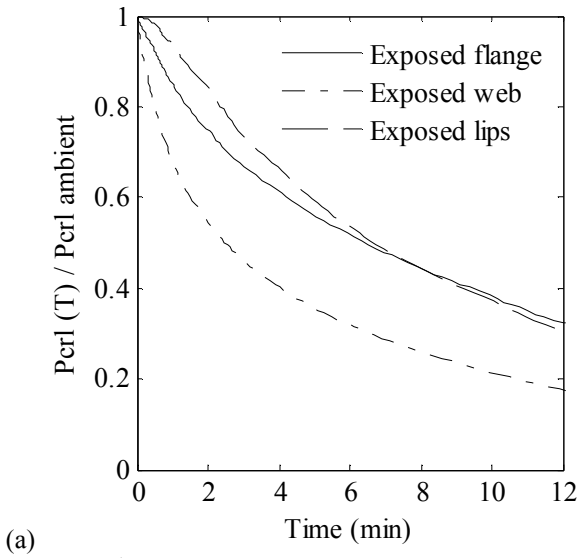

(a)

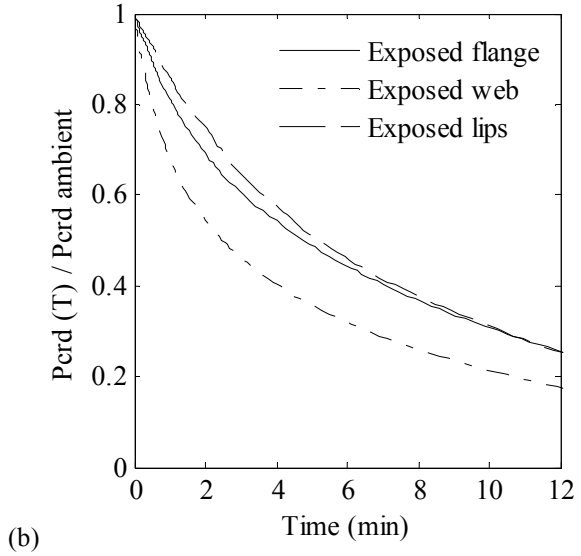

(b)

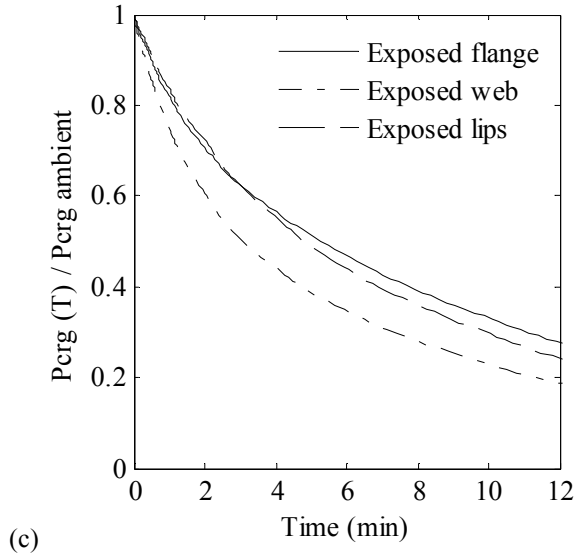

(c)

Figure 10: Normalized (a) local, (b) distortional and (c) global buckling loads with respect to the ambient critical loads, and buckling modes for different fire exposure conditions

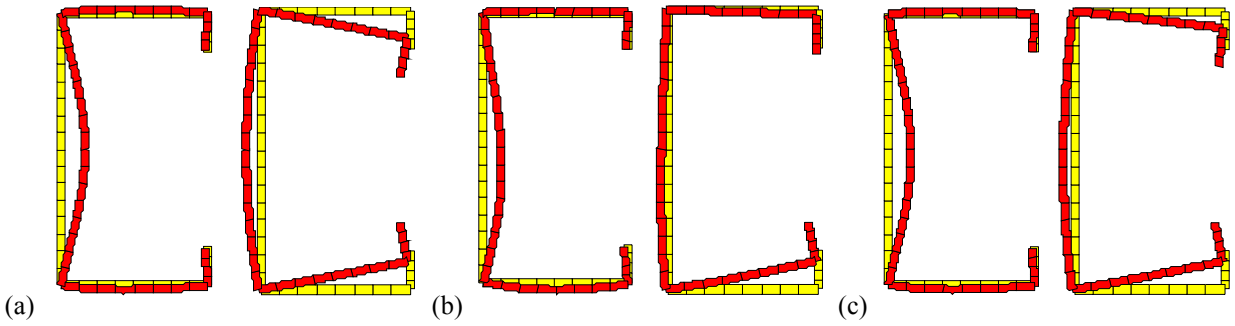

Figure 11: Local and distortional mode shapes (left and right) at (a) 0, (b) 12 and (c) 36 minutes of fire exposure on the bottom flange

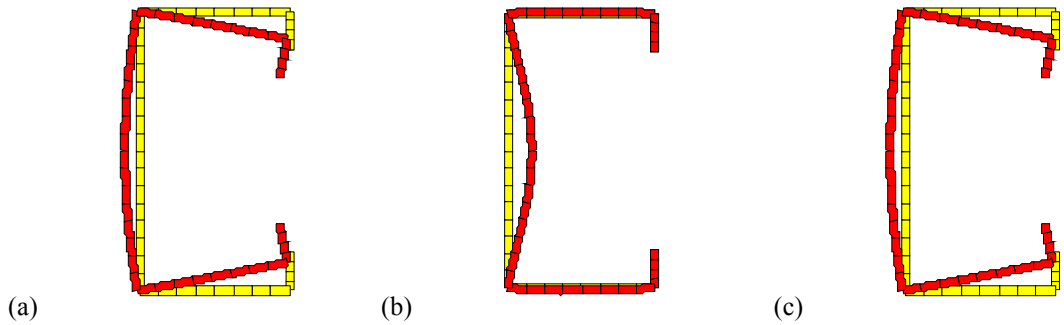

Figure 12: Mode shapes corresponding to the minimum buckling load from (a) 0 to 16 minutes, (b) 16 to 24 minutes and (c) after 24 minutes of fire exposure on the web

5. Material and geometric nonlinear analysis

In addition to exploring the elastic buckling analysis, full nonlinear response of the 250S137-68 [345 MPa, 50 ksi] is also studied. The two response regimes of interest are (1) the mechanical deformations associated with the thermal (fire) demands, often referred to as thermal bowing, and (2) the axial collapse capacity of the thermally deformed cross-section under axial load. The nonlinear mechanical response includes both material and geometric nonlinearity.

The material nonlinearity is captured through typical metal plasticity with von Mises yield criterion and isotropic hardening. The nonlinear material response is elastic, $E(T)$, plastic, $F_y(T)$ (where T denotes the temperature dependence in the model), with temperature dependent stress-plastic strain relationships based on experimental results, shown in Fig. 5 (from Kankanamge and Mahendran 2011). Here the analysis is sequential, so the material nonlinearity is implemented after a certain time of exposure to fire, thus the material parameters vary depending on the temperature distribution in the section. Residual stresses are ignored, consistent with available modeling guidance at ambient temperatures (Schafer and Peköz 1998, Schafer et al. 2010) and under fire (Ranawaka and Mahendran 2010).

Geometric nonlinearity is also captured in the model and may be initialized by utilizing a deformed (imperfect) geometry. The characterization of local, distortional, and global imperfections in CFS members at ambient temperatures is provided by Zeinoddini and Schafer

(2012). However, the mechanical deformations associated with thermal (fire) demands, particularly when they are realistic and non-uniform, creates its own "imperfections". Studies at elevated temperatures have demonstrated only a weak sensitivity to initial ambient temperature imperfections (Feng et al. 2003b), but have recommended the use of artificially large geometrical imperfections (e.g., global at L/500) based on eigenmodes (Kaitila 2002). In this initial work, ambient temperature imperfections are ignored and instead the deformed geometry for the non-uniform thermal demand is generated and assumed to dominate. Future work will explore the interaction between ambient and temperature-based (thermal bowing) imperfections and their impact on predicted capacities.

5.1 Thermal bowing

Bare CFS members have fast heating rates when exposed to fire due to the high thermal conductivity of steel and the high section factors of thin-walled members. The temperature response is significantly modified when isolation (e.g. gypsum) boards are used. The board creates a relatively high thermal gradient through the cross-section. For instance, the temperature difference between the exposed and unexposed faces of CFS studs in wall systems with gypsum boards has reached ~400ºC during experiments (Feng and Wang 2005). This temperature difference can result in differential strains for the two flanges and the resulting member deformation (bending) is commonly referred to as thermal bowing. Thermal bowing may induce additional bending moments to the structural members.

Thermal deflections may be simplified to pure thermal bowing, assuming only beam bending deformations (no cross-section or shear deformations), linear temperature variation across the depth (d) of the section, and a constant coefficient of thermal expansion (α). Under simply supported end conditions the maximum (mid-height) thermal bowing of a member of length L is:

$$\delta_{\max} = \frac{\alpha \Delta T L^2}{8d} \tag{1}$$

where ΔT is the temperature difference between the flanges. Eq. 1 generally gives a good approximation of the thermal deflection expected in the major axis of a compression member with one flange directly exposed to fire (see Fig. 13), even though the temperature variation from heat transfer analysis may be slightly nonlinear. The expected thermal deflection is about L/200, which is five times larger than the typical global imperfection at ambient conditions (i.e. L/1000).

In axial compression thermal bowing is magnified by second order (P-δ) effects and the degradation of mechanical properties. Approximating the P-δ effects and considering neutral axis shift (e_y) Feng and Wang (2005) provided an improved version of Eq. 1 for thermal bowing:

$$y_{\max} = \frac{2\alpha \Delta TPL/3d}{64EI/L^3 - 16P/3L} + \frac{\alpha \Delta T L^2}{8d} - e_y \tag{2}$$

where P is the axial load and EI the major-axis bending rigidity. Eq. (2) may be expressed as a magnification of δ_{max} from Eq. (1):

$$y_{\max} = M\delta_{\max} - e_y \tag{3}$$

$$\text{where } M = \frac{EI/PL^2}{EI/PL^2 - 1/12}, \text{ and } 1/12 < EI/PL^2 \le 21/12 \tag{4}$$

As provided in Eq. (4), the magnification is a modified version of the typical P-δ amplification (i.e., B_1 factor in AISC, $(EI/L^2)/P \propto P_{cr}/P$).

Feng and Wang (2005) assumed a constant thermal expansion coefficient, but thermal strains are temperature dependent and consequently the thermal expansion coefficient is not constant. Proposed models for α range from constant to nonlinear, as shown in Fig. 14. Interestingly Wei and Jihong (2012) showed that at about 650ºC to 750ºC thermal strains remain fairly constant despite further temperature increase. For this temperature range, the thermal expansion coefficient approaches zero. However, this phenomenon is associated with a phase transformation in the chemical structure of the steel and generally not relevant for structural response.

Even though the thermal gradient along the unexposed flange is small, thermal deflections perpendicular to the minor axis are developed. This effect is more significant when nonlinear models of thermal expansion coefficient are adopted (see Fig. 15). Deflections perpendicular to the minor axis have typically been ignored, but may be significant, particularly when utilizing the model proposed by Wei et al. (2012), which was developed from experimental results on CFS specimens under transient state conditions. For fully non-uniform fire demands, and including the thermal demands developed through heat-transfer through the fasteners, thermal deformations sympathetic to cross-section buckling such as local and distortional buckling are also possible, and worthy of future study.

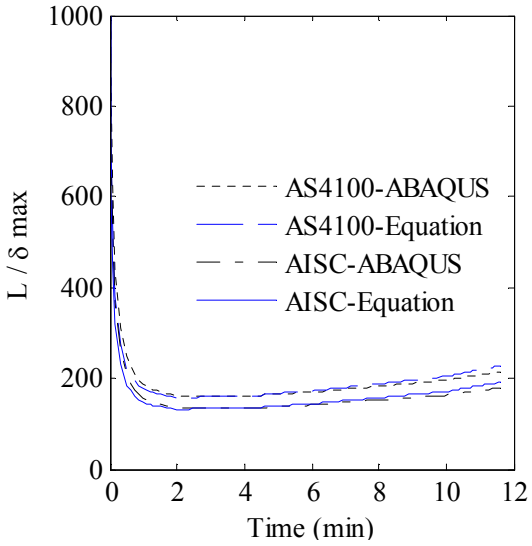

Figure 13: Thermal bowing perpendicular to the major axis of a lipped channel section using Eq. 1 and Abaqus, both with constant thermal expansion coefficients from AS4100 and AISC

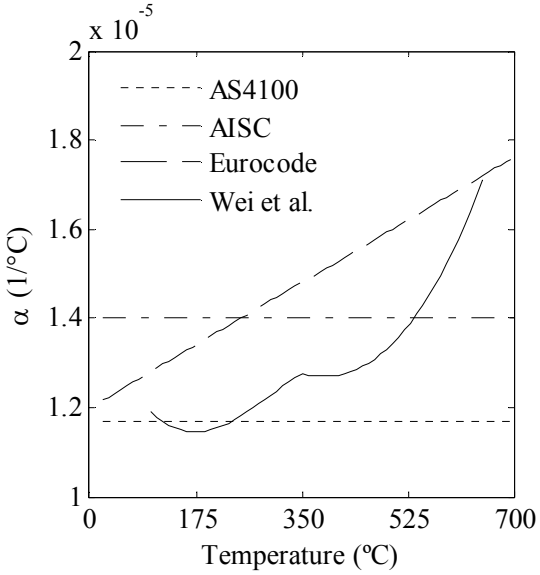

Figure 14: Thermal expansion coefficient models

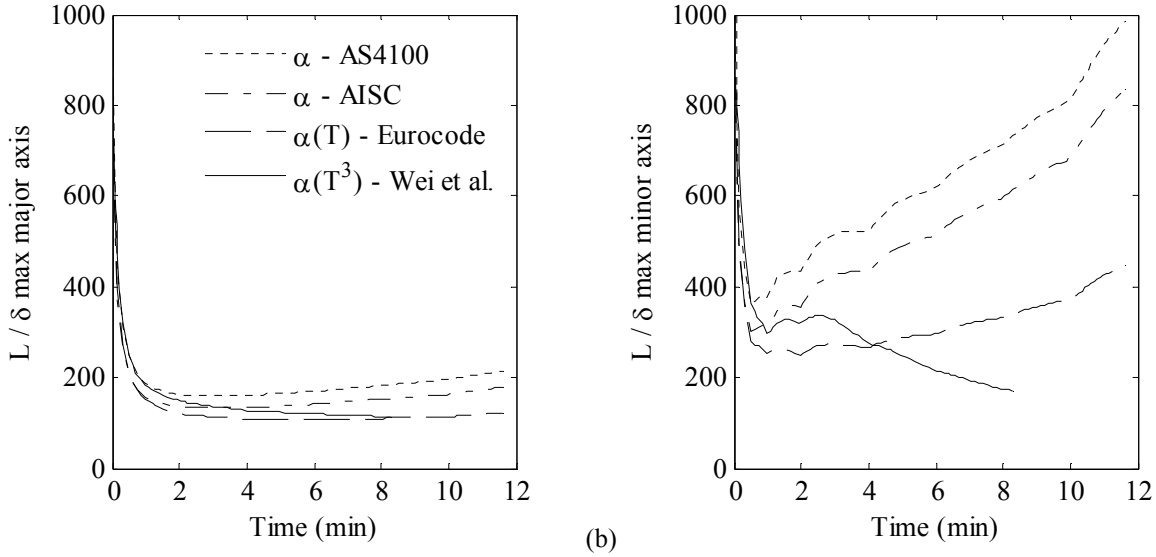

Figure 15: Thermal bowing perpendicular to the (a) major axis and (b) minor axis of a lipped channel section using constant (AS4100 and AISC), linear (Eurocode 3) and nonlinear (Wei et al. 2012) thermal expansion coefficients

5.2 Collapse under axial load

To explore collapse behavior under fire, a fully material and geometric nonlinear analysis was conducted on the 250S137-68 after it have been subjected to given times of fire exposure (i.e. the Standard fire curve), assuming heating on one flange (temperature distribution of Fig. 9-a). Heat analysis was used to determine the temperature field (T) at time (t). Thermal-mechanical analysis at (t,T) was used to determine deflections that equilibrate the section, and serve as the initial "imperfection" in the subsequent collapse analysis under a uniform compressive displacement. The degradation of the axial capacity as predicted from the collapse analysis is provided in Fig. 16. Qualitatively, the degradation follows the same trends as the elastic buckling degradations as previously discussed.

Currently, the authors are investigating a variety of design methods related to DSM to accurately capture this strength degradation. Chief among the issues being considered are whether or not the thermal bowing requires explicit consideration as a beam-column (or may be smeared into an equivalent imperfection), and how to handle mode interactions not observed at ambient temperatures. In addition, the authors are expanding the parametric studies to include a wider variety of cross sections and fire scenarios.

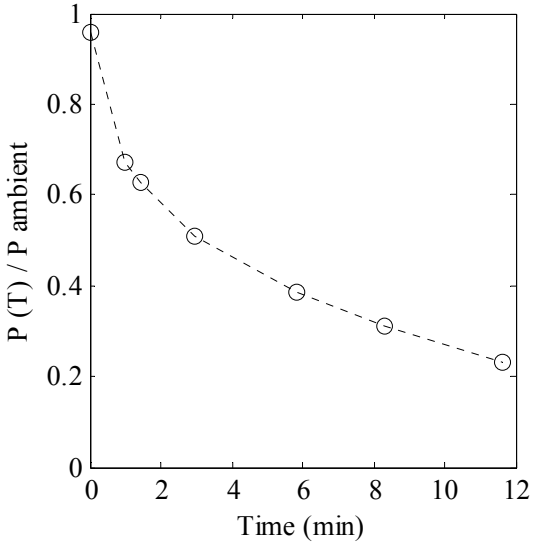

Figure 16: Degradation of the axial capacity of a 250S137-68 CFS compression member under thermal gradient through nonlinear analyses

4. Conclusions

The capacity of a compression member under fire can be defined according to the amount of time it can withstand the axial load and the magnitude of such load. Therefore, it is necessary to associate fire resistance and load carrying capacity. This paper provides computational results for critical elastic local, distortional and global buckling loads as a function of fire exposure, for a particular fire scenario, considering temperature dependent material properties and shift of the center of resistance due to thermal action. Results show that buckling loads decrease with increasing temperature, and the rate of degradation varies according to the fire scenario. Also, modal interaction absent at ambient temperature can be significant when thermal gradients are developed. Elastic buckling loads computed through the finite element method (using Abaqus) and finite strip method (using CUFSM) are comparable. Thus, the more time efficient finite strip solution is preferred. In the future, these time-dependent (or temperature-dependent) critical loads can be utilized to compute the ultimate strength by design methods (e.g. Direct Strength Method). Future research aims to characterize the squash load for thin-walled CFS members under thermal gradients, and study the effect of geometric imperfections and thermal deflections on the load-carrying capacity under realistic fire conditions. This study seeks to develop robust DSM-based equations to predict load-carrying capacity related to fire resistance of CFS members.

Acknowledgments

The authors wish to thank Prof. Yared Shifferaw and Dr. Zhanjie Li for helping to develop the code to generate Abaqus input files.

References

Abaqus (2009). "Abaqus Analysis User's Manual 6.9-EF." Hibbitt, Karlsson & Sorensen, Inc., Pawtucket, Rhode Island.

AISC (2008). "Steel Construction Manual." Thirteenth Edition, in Appendix 4: Structural Design for Fire Conditions, United States of America.

AISI-S200 (2007), "North American Standard for Cold-Formed Steel Framing – General Provisions". American Iron and Steel Institute.

Alfawakhiri, F., Sultan M.A., (2001). "Numerical modelling of steel members subjected to severe thermal loads." *National Research Council Canada, NRCC-44225*.

Almeida, S.J.C., Rodriguez, J.P. Neto, J.M. (2012). "Behaviour of compressed cold formed steel elements at high temperatures." *Proceedings of the 7th International Conference on Structures in Fire*, Switzerland.

Chen, J., Young, B. (2006). "Design of cold-formed steel lipped channel columns at elevated temperatures." *Proceedings of the International Colloquium on Stability and Ductility of Steel Structures*, Lisbon, Portugal. 737-746.

Chen, J., Young, B. (2007). "Experimental investigation of cold-formed steel material at elevated temperatures". *Thin-Walled Structures*, 45(2007) 96-110.

Clark, C. L. (1953). "High-temperature alloys." New York, London: Pitman.

Collette, K.A. (2007). "Comparisons of Structural Designs in Fire." M.Sc. Thesis, Worcester Polytechnic Institute.

Committee of European Standardization (CEN) ENV 1993-1-2. "Eurocode 3; Design of steel structures, Part1.2: General rules, Structural fire design".

Costes, F. (2004). "Modélisation thermomécanique tridimensionnelle par éléments finis de la coulée continue d'aciers." Ph.D. Thesis, École des Mines de Paris.

Feng, M., Wang, Y.C., Davies, J.M. (2003a). "Structural behavior of cold-formed thin-walled short steel channel columns at elevated temperatures, Part 1: experiments." *Thin-Walled Structures*, 41(2003) 543–570.

Feng, M., Wang, Y.C., Davies, J.M. (2003b). "Structural behavior of cold-formed thin-walled short steel channel columns at elevated temperatures, Part 2: Design calculations and numerical analysis". *Thin-Walled Structures*, 41(2003) 571–594.

Feng, M., Wang, Y.C., Davies, J.M. (2003c). "Axial strength of cold-formed thin-walled steel channels under non-uniform temperatures in fire." *Fire Safety Journal*, 38(2003) 679-707.

Feng, M., Wang, Y. C. (2005). "An analysis of the structural behaviour of axially loaded full-scale cold-formed thin-walled steel structural panels tested under fire conditions." *Thin-Walled Structures,* 43(2005) 291-332.

Gerlich, J.T. (1995). "Design of Loadbearing light steel frame walls for fire resistance". *Fire Engineering research Report 95/3*, University of Canterbury.

ISO, "International Organization for Standardization (ISO), International Standard, Fire Resistance Tests of Elements in Building Construction, ISO-834-1." Switzerland, 1999.

Kaitila, O. (2002). "Finite element modelling of cold-formed steel members at high temperatures." Thesis for the Degree of Licentiate of Science in Technology, Helsinki University of Technology, Laboratory of Steel Structures, Publications 24.

Kankanamge, N.D., M. Mahendran (2011). "Mechanical properties of cold-formed steels at elevated temperatures". *Thin-Walled Structures*, 49(1) 26-44.

Kodur, V.R., Sultan, M.A. (2001). "Factors governing fire resistance of loadbearing steel stud walls." National Research Council Canada, NRCC-45211.

Lee, J. (2004). “Local buckling behaviour and design of cold-formed steel compression members at elevated temperatures.” Ph.D. Thesis, Brisbane, Australia: Queensland University of Technology.

Li, Z., Batista Abreu, J.C., Ádány, S., Schafer, B.W. (2012). “Cold-formed steel member stability and the constrained finite strip method.” *The 6th International Conference on Coupled Instabilities in Metal Structures*. Scotland, UK

Luecke, W.E., McColskey, J.D., McCowan, C.N., Banovic, S.W., Fields, R.J., Foecke, T., Siewert, T.A., Gayle, F.W. (2005). "Mechanical Properties of Structural Steels". *Federal Building and Fire Safety Investigation of the World Trade Center Disaster, NIST NCSTAR 1-3D,* Washington, DC

Ranawaka, T., Mahendran, M. (2010). “Numerical modelling of light cold-formed steel compression members subjected to distortional buckling.” *Thin-Walled Structures*, 48(2010) 334–344.

Schafer, B.W., Ádány, S. (2006). “Buckling analysis of cold-formed steel members using CUFSM: conventional and constrained finite strip methods.” *Eighteenth International Specialty Conference on Cold-Formed Steel Structures*, Orlando, FL.

Schafer, B.W., Li, Z., Moen, C.D. (2010). “Computational modeling of cold-formed steel.” Elsevier, Thin-walled Structures. 48 (10-11) 752-762. (doi:10.1016/j.tws.2010.04.008)

Schafer, B.W., Peköz, T. (1998). “Computational Modeling of Cold-Formed Steel: Characterizing Geometric Imperfections and Residual Stresses.” Elsevier, Journal of Constructional Steel Research. 47 (3) 193-210. (doi:10.1016/S0143-974X(98)00007-8)

Shahbazian, A., Wang, Y.C. (2011a). “Application of the Direct Strength Method to local buckling resistance of thin-walled steel members with non-uniform elevated temperatures under axial compression.” *Thin-Walled Structures*, (49) 1573-1583.

Shahbazian, A., Wang, Y.C. (2011b). “Calculating the global buckling resistance of thin-walled steel members with uniform and non-uniform elevated temperatures under axial compression.” *Thin-Walled Structures*, (49) 1415-1428.

Shahbazian, A., Wang, Y.C. (2012). “Direct Strength Method for calculating distortional buckling capacity of cold-formed thin-walled steel columns with uniform and non-uniform elevated temperatures.” *Thin-Walled Structures*, (53) 188-199.

Standards Australia (1998). “AS4100-1998 Steel structures.” Sydney, Australia.

Wei, C., Y. Jihong (2012). "Mechanical properties of G550 cold-formed steel under transient and steady state conditions." *Journal of Constructional Steel Research,* 73(0) 1-11.

Zeinoddini, V.M., Schafer, B.W. (2012). “Simulation of geometric imperfections in cold-formed steel members using a spectral representation approach.” Elsevier, Thin-walled structures. 105-117 (DOI: 10.1016/j.tws.2012.07.001)